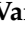





## Article

# Peptidases Are Potential Targets of Copper(II)-1,10-Phenanthroline-5,6-dione Complex, a Promising and Potent New Drug against *Trichomonas vaginalis*

Graziela Vargas Rigo <sup>1</sup>, Fernanda Gomes Cardoso <sup>1</sup>, Matheus Mendonça Pereira <sup>2</sup>, Michael Devereux <sup>3</sup>, Malachy McCann <sup>4</sup>, André L. S. Santos <sup>5</sup> and Tiana Tasca <sup>1,\*</sup>

- <sup>1</sup> Faculdade de Farmácia and Centro de Biotecnologia, Universidade Federal do Rio Grande do Sul, Porto Alegre 90610-000, RS, Brazil; grazivrigo@gmail.com (G.V.R.); fe12gomes@outlook.com (F.G.C.)
- <sup>2</sup> CIEPQPF, Department of Chemical Engineering, University of Coimbra, Rua Sílvio Lima, Pólo II—Pinhal de Marrocos, 3030-790 Coimbra, Portugal; matheus@eq.uc.pt
- <sup>3</sup> The Inorganic Pharmaceutical and Biomimetic Research Centre, Focas Research Institute, Dublin Institute of Technology, D08 CKP1 Dublin, Ireland; michael.devereux@dit.ie
- <sup>4</sup> Chemistry Department, Maynooth University, National University of Ireland, W23 F2H6 Maynooth, Ireland; malachy.mccann@mu.ie
- <sup>5</sup> Laboratório de Estudos Avançados de Microrganismos Emergentes e Resistentes (LEAMER), Departamento de Microbiologia Geral, Instituto de Microbiologia Paulo de Góes, Universidade Federal do Rio de Janeiro, Rio de Janeiro 21941-902, RJ, Brazil; andre@micro.ufrj.br
- \* Correspondence: tiana.tasca@ufrgs.br

**Abstract:** *Trichomonas vaginalis* is responsible for 156 million new cases per year worldwide. When present asymptotically, the parasite can lead to serious complications, such as development of cervical and prostate cancer. As infection increases the acquisition and transmission of HIV, the control of trichomoniasis represents an important niche for the discovery and development of new antiparasitic molecules. This urogenital parasite synthesizes several molecules that allow the establishment and pathogenesis of infection. Among them, peptidases occupy key roles as virulence factors, and the inhibition of these enzymes has become an important mechanism for modulating pathogenesis. Based on these premises, our group recently reported the potent anti-*T. vaginalis* action of the metal-based complex [Cu(phenidione)<sub>3</sub>](ClO<sub>4</sub>)<sub>2</sub>·4H<sub>2</sub>O (Cu-phenidione). In the present study, we evaluated the influence of Cu-phenidione on the modulation of proteolytic activities produced by *T. vaginalis* by biochemical and molecular approaches. Cu-phenidione showed strong inhibitory potential against *T. vaginalis* peptidases, especially cysteine- and metallo-type peptidases. The latter revealed a more prominent effect at both the post-transcriptional and post-translational levels. Molecular Docking analysis confirmed the interaction of Cu-phenidione, with high binding energy (−9.7 and −10.7 kcal·mol<sup>−1</sup>, respectively) at the active site of both TvMP50 and TvGP63 metallopeptidases. In addition, Cu-phenidione significantly reduced trophozoite-mediated cytolysis in human vaginal (HMVII) and monkey kidney (VERO) epithelial cell lineages. These results highlight the antiparasitic potential of Cu-phenidione by interaction with important *T. vaginalis* virulence factors.

**Keywords:** *Trichomonas vaginalis*; metallopeptidases; cytolysis; proteolytic activity; copper-phenidione



**Citation:** Rigo, G.V.; Cardoso, F.G.; Pereira, M.M.; Devereux, M.; McCann, M.; Santos, A.L.S.; Tasca, T. Peptidases Are Potential Targets of Copper(II)-1,10-Phenanthroline-5,6-dione Complex, a Promising and Potent New Drug against *Trichomonas vaginalis*. *Pathogens* **2023**, *12*, 745. <https://doi.org/10.3390/pathogens12050745>

Academic Editor: Timothy G. Geary

Received: 23 March 2023

Revised: 9 May 2023

Accepted: 17 May 2023

Published: 22 May 2023



**Copyright:** © 2023 by the authors. Licensee MDPI, Basel, Switzerland. This article is an open access article distributed under the terms and conditions of the Creative Commons Attribution (CC BY) license (<https://creativecommons.org/licenses/by/4.0/>).

## 1. Introduction

Trichomoniasis is among the most common non-viral sexually transmitted infectious diseases. It is caused by the widespread obligate extracellular parasitic protozoan *Trichomonas vaginalis*. According to the World Health Organization (WHO), approximately 156 million new cases of trichomoniasis are reported worldwide per year [1]. Although many cases remain asymptomatic, patient complaints include the presence of itching, discharge, and local inflammation [2]. In addition, the presence of the parasite can lead to serious complications generated by the production of key molecules (e.g., different classes

of extracellular hydrolytic enzymes) that allow the establishment and pathogenesis of infection. For example, *T. vaginalis* genome sequencing has demonstrated the presence of 440 peptidases' coding genes responsible for composing the degradome of *T. vaginalis*, acting in both physiological and pathological events that culminate in a successful infectious process. In general, peptidases are hydrolytic enzymes able to cleave peptide bonds in peptides/proteins, and are classified depending on the amino acid/metal present in their catalytic site that is responsible for binding and cleaving proteinaceous substrates [3].

*Trichomonas vaginalis* peptidases are classified as cysteine (total of 220 genes), metallo (123 genes), serine (80 genes), threonine (17 genes), and aspartic (6 genes) peptidases. Metallo (MP) and cysteine (CP) peptidases are responsible for more than half of proteolytic diversity in *T. vaginalis* [4]. CPs have about seven clans composed of fourteen families, including papain (C1), calpain (C2), ubiquitin hydrolases (C12 and C19), and metacaspases (C14), among others [4]. Importantly, representatives of CPs are responsible for the degradation of secretory leukocyte protease inhibitor, a substance involved in human immunodeficiency virus (HIV) protection by inhibiting the entry of the virus into monocyte cells, making trichomoniasis a facilitating agent for HIV acquisition [5]. MPs are hydrolases that require the presence of a metal to perform the cleavage of peptide bonds in the target substrates. In *T. vaginalis*, eight clans containing fourteen families have been described, including leishmanolisin (or gp63) peptidases (M8), FtsH endopeptidases (M41), and several families of aminopeptidases, such as P aminopeptidases (M24) [4]. In general, peptidases are ubiquitously found in living organisms and are responsible for several vital functions in microbial cells, including nutrition, proliferation, growth, differentiation, and signaling, as well as pathological functions such as adhesion events, escape, dissemination, and immunomodulation [6,7]. Moreover, the microhabitat has been shown to play a potential role in the selection of certain functions related to peptidases. Different peptidases in *T. vaginalis* have been identified in the parasite secretome, such as subtilisin serine peptidases (S8), papain-type CPs, and MPs of the families M8 and M24 [8].

According to Arroyo [9], 123 genes encoding MPs have been described in *T. vaginalis*. TvMP50 and TvGP63 are most known MPs in trichomonads, both contributing to host cell damage. TvMP50 is an immunogenic MP detected during trichomoniasis in serum samples from male patients. The activity of this enzyme is mediated by  $Zn^{2+}$ , which is present in high levels in the male urogenital microenvironment, being considered part of the group of cytolytic effectors involved in the pathogenicity of *T. vaginalis* mediated by environmental conditions [10,11]. TvGP63 is a family of enzymes that has 48 members, of which 37 members are transmembrane proteins; its activity has been related to cytotoxicity to HeLa cell monolayers [12,13]. Considering the participation of peptidases in the pathogenesis and virulence of trichomoniasis, these enzymes stand out as promising targets for the development of new anti-*T. vaginalis* therapies.

The compound 1,10-phenanthroline-5,6-dione (phendione) has been the focus of several biological studies due to its favorable chemical and pharmacological versatility [14–16]. The antibacterial effects of phendione and its silver and copper derivatives have been reported against the widespread multidrug-resistant gram-negative bacterium *Pseudomonas aeruginosa*, revealing that elastase B (a metallo-type peptidase that is a well-known virulence factor of this pathogen) is a target of these metal-based complexes [14,17]. In addition, these complexes have displayed antiparasitic activity against protozoa such as *Leishmania amazonensis*, *Leishmania braziliensis*, *Leishmania chagasi*, and *T. vaginalis* [16,18,19]. Interestingly, the interaction of copper(II) and silver(I)-phendione compounds with MPs have been described as key target in its antiparasitic activity [16]. In this context, phendione-based compounds were able to inhibit the main metallopeptidase activity (gp63) produced by *L. brasiliensis* promastigotes, affecting either the infection establishment or infection maintenance processes between parasites and macrophages [16]. Moreover, Cu-phendione induced several impacts on metabolic activity and membrane potential parameters of these *Leishmania* species [19]. Similarly, our group previously demonstrated the potent action of phendione and its silver and copper complexes against *T. vaginalis*, especially the copper

derivative (Cu-phendione), which presented values of minimum inhibitory concentration comparable to metronidazole, a common drug used in clinical therapy [18]. Furthermore, Cu-phendione and metronidazole acted synergistically in order to more effectively kill *T. vaginalis* trophozoites [18]. In addition, we showed that Cu-phendione killed *T. vaginalis* through redox homeostasis imbalance and apoptosis, a mode of action that is quite distinct from that caused by metronidazole [20].

Considering the promising contribution of phendione and its silver and copper derivatives in the prospection of therapeutic alternatives against trichomoniasis, as well as the interaction of these compounds with MPs produced by clinically relevant parasites, in the present study we investigated the effect of phendione and its metal-based complexes against *T. vaginalis* peptidases. Through evaluation of enzyme function and gene expression, significant disturbance in the proteolytic pathway was observed after parasite treatment with Cu-phendione. These data were corroborated by *in silico* approaches using TvMP50 and TvGP63 as *T. vaginalis* MP models. Finally, a cytoprotective effect was observed during the interaction process between *T. vaginalis* and both vaginal and renal epithelial cells induced by Cu-phendione treatment.

## 2. Materials and Methods

### 2.1. Parasites

The *T. vaginalis* isolate ATCC 30236 was used in this study, and was cultivated in trypticase-yeast extract-maltose (TYM) medium, pH 6.0, supplemented with 10% adult bovine serum and maintained at 37 °C [21]. Organisms in the logarithmic phase of growth exhibiting normal morphology and motility were counted in a hemocytometer using trypan blue exclusion dye (0.2%), then the parasitic density was adjusted to  $2 \times 10^5$  trophozoites/mL. All experiments were conducted in triplicate with at least three independent cultures ( $n = 3$ ). To evaluate the cytotoxicity of parasites against mammalian cells, the fresh clinical isolates TV-LACM15, TV-LACM22, and TV-LACH4 were cultivated as described above. The fresh clinical isolates were obtained from urine and vaginal discharge and maintained under cryopreservation (UFRGS Research Ethical Committee approved the assays under authorization number 18923).

### 2.2. Treatment

Cu-phendione was prepared in accordance with the methods previously described by McCann et al. [22]. Treatment occurred by exposing trophozoites ( $2 \times 10^5$  trophozoites/mL) to Cu-phendione at MIC value for 2 h. The minimal inhibitory concentration (MIC) value for TV-ATCC 30236 and TV-LACH4 was 12.5  $\mu$ M, while for TV-LACM15 and TV-LACM22 it was 6.25  $\mu$ M [18]. For all analyses, control condition refers to trophozoites grown in culture medium without Cu-phendione.

### 2.3. Computational Analysis of TvMP50, TvGP63, and TvCP2

The amino acid sequences of TvMP50 (TVAG\_403460) (MEROPS: MER0082185; uniprot: A2F8Y2; genbank: EAX98664) and TvGP63 (TVAG\_367130) (MEROPS: MER0078144, uniprot: A2G9D5, genbank: EAX86230.1) were submitted to AlphaFold2 software for prediction of three-dimensional structure [23]. The TvCP2 predicted structure was obtained from the AlphaFold Protein Structure Database (uniprot: Q27107). Subsequently, the protonation states of the titrable residues of TvMP50, TvGP63, and TvCP2 were calculated using ProteinPrepare (PlayMolecule web server—playmolecule.org, accessed on 11 November 2022) [24]. The MP PDB file obtained through AlphaFold was uploaded to the ProteinPrepare tool. pKa calculation was performed at pH 4.0 to 7.0 for TvMP50 and TvGP63 and at pH 6.0 for TvCP2 without water molecules and ligands from the input PDB file. After the calculation, protonated PDB files were analyzed. The electrostatic surface properties were calculated using sequential calculation for multi-network focusing of automatic concentration in Adaptive Poisson-Boltzmann Solver (APBS).

The interaction of TvMP50 and TvGP63 with ligands (1,10-phenanthroline, phendione, Ag-phendione and Cu-phendione) and of TvCP2 with Cu-phendione were identified using the AutoDock Vina 1.1.2 program [25]. The predicted structures were prepared as described in the above, using pH 6.0, and subjected to molecular docking analysis. Auto DockTools (ADT) [26] was used to prepare the TvMP50, TvGP63, and TvCP2 file as a receptor. The atomic coordinates (3D) of the ligands were created using Discovery Studio v20 (Accelrys, San Diego, CA, USA) with the Chem3D-MM2 protocol applied for energy minimization (Chem3D Ultra, CambridgeSoft Co., 100 Cambridge Park Drive, Cambridge, MA, USA, 02140), and the rigid root of each ligand was generated using AutoDockTools (ADT). The center of the gridbox in the TvMP50 center of mass was  $-0.101 \times 0.399 \times -1.521$ , while for TvGP63 it was  $-4.804 \times 2.156 \times 0.008$  and for TvCP2 it was  $-2.691 \times 0.922 \times 18.558$  on the x-, y-, and z-axes, respectively. The gridbox size (Å) was  $90 \times 60 \times 80$  for TvMP50,  $110 \times 100 \times 80$  for TvGP63, and  $60 \times 60 \times 90$  for TvCP2. The binding model with lowest free binding energy was researched from among ten different conformers for each ligand. Metallopeptidase and ligands complexes were visualized and analyzed using Discovery Studio, v20 (Accelrys, San Diego, CA, USA).

#### 2.4. Proteolytic Activity Assay

*T. vaginalis* proteolytic activity was evaluated according to Weber et al. [27] using azocasein as substrate. After treatment, protein quantification was performed by the Coomassie blue method [28] and adjusted to a final concentration of 0.3 mg/mL. The assay was conducted in 0.1 M Tris-HCl, pH 7.0, for 90 min at 37 °C with 2% azocasein (Sigma-Aldrich, Co. St. Louis, CA, USA). The reaction was interrupted with 10% trichloroacetic acid and, after centrifugation at  $10,000 \times g$  for 5 min, 1.8 N NaOH was added to the supernatants. Absorbance was measured at 420 nm and azocasein degradation of treated organisms was compared to control, with 100% peptidase activity. Furthermore, the cleavage over two specific peptide substrates, Z-Phe-Arg-AMC at 10 µM (Z-Phe-Arg 7-amido-4-methylcoumarin hydrochloride, Sigma-Aldrich) and DNP-Pro-Leu-Gly-Met-Trp-Ser-Arg at 25 µM (MMP2/MMP9 substrate, Sigma-Aldrich), was tested in order to evaluate the CP and MP activities, respectively. The substrates' cleavage was evaluated in a spectrofluorometer (SpectraMax Gemini XPS, Molecular Devices, San Jose, CA, USA) using an excitation/emission wavelength of 280/360 nm for MP and 380/460 nm for CP. The reactions were initiated with the addition of 10 µg of protein and the proteolytic inhibitors tested were 1,10-phenanthroline (5 mM) and E-64 (*N-trans*-epoxysuccinyl-L-leucine-4-guanidinobutylamide) (10 µM).

#### 2.5. Sodium Dodecyl Sulfate–Polyacrylamide Gel Electrophoresis (SDS-PAGE) Assay

The peptidase profile of *T. vaginalis* was assayed by gel electrophoresis containing 1% gelatin as proteinaceous substrate incorporated into the sodium dodecyl sulfate-polyacrylamide gel [17]. Trophozoites' cellular protein was adjusted to 60 µg/mL of protein using the Coomassie method and then loaded in the slot [28]. After electrophoresis at a constant voltage (120 V) at 4 °C, 2.5% Triton X-100 was used to remove SDS. Afterwards, gel was added into digestion buffer comprising 50 mM phosphate buffer, pH 5.5, for 24 h at 37 °C. The gels were stained for 2 h with 0.2% Coomassie brilliant blue R-250 in methanol:acetic acid:water (50:10:40) and destained in a solution containing methanol:acetic acid:water (5:10:85). Low molecular mass standards (Sigma-Aldrich) were used for comparison of molecular masses.

#### 2.6. Mass Spectrometry Analysis

The decrease in proteolytic activity modulation was observed in the gel, then the peptidases related to this region were determined by mass spectrometry analysis. The gel was digested as described by Martineli et al. [29]. The obtained peptides were submitted to reverse phase chromatography (Nano Acquity Ultra Performance LC-UPLC® (Waters, Milford, MA, USA)) using a Nanoease C18, 75 µm ID at 35 °C. Elution occurred in a



constant flow ramp of 0 to 60% acetonitrile in 0.1% trifluoroacetic acid at 0.6 nL/min. The analysis was performed on a G2-XS Q-TOF Xevo mass spectrometer<sup>®</sup> and the identification was based on the genome database of *T. vaginalis* (*T. vaginalis* G3, G3; ATCC PRA-98, WGS project AAHC01000000) held on the *ProteinLynx Global Server* (PLGS) platform version 2.2.5 and Uniprot database (<https://www.uniprot.org/>, accessed on 9 November 2019).

### 2.7. Expression of mRNA through qRT-PCR

Evaluation of the relative gene expression of *T. vaginalis* peptidases was performed for the CPs (calpain, cathepsin L and B), MPs (TvMP50 and TvGP63), and aspartic-type peptidase (cathepsin D) [13,27]. Quantitative real-time PCR (qRT-PCR) was used to compare the mRNA levels expressed between trophozoites treated with Cu-phendione and the control without treatment. RNA extraction was performed with TRIzol [30] and analyzed with a Thermo Scientific NanoDrop 1000<sup>®</sup> spectrophotometer, using only samples with adequate purity. To standardize the primer curves, we used cDNA produced through a High-Capacity cDNA Reverse Transcription Kit (Applied Biosystems). The analyses were performed according to Santos et al. [31] using the DNA topoisomerase II as reference gene. The GoTaq<sup>®</sup> 1-step RT-qPCR reaction system was prepared with 5 µL of 2 GoTaq<sup>®</sup> qPCR Master Mix, 0.2 µL of GoScript<sup>™</sup> RT Mix, 0.1 or 0.2 µM of primer, and 2X µL RNA (5.0 ng). The conditions used for amplification and detection of the gene were activation of the enzyme at 95 °C for 10 min followed by 40 cycles composed of 95 °C for 10 s. The melting curve was performed by increasing the temperature from 60, 64, and 68 °C to 95 °C with 1 °C for 5 s. The peptidases, primer concentrations, and ideal annealing temperature are described in Table 1. Analysis of the relative expression of the genes was performed through Rotor-Gene Q series 2.1 software; the reference gene value ( $\Delta\text{Ct}$ ) was used for threshold (Ct) cycles and compared to the control ( $\Delta\Delta\text{Ct}$ ), with values expressed as  $2^{-\Delta\Delta\text{Ct}}$ .

**Table 1.** Parameters used for qRT-PCR of *Trichomonas vaginalis* peptidases.

Identification	Primers (5'-3')	Primer Concentration	Annealing Temperature (°C)
<b>Calpain (TVAG_161170)</b>	F: CCA AAG GAT GCA CGA ATT TT R: GCG GAC ATT AGC TGG TTT GT	0.2	60
<b>Cathepsin L (TVAG_057000)</b>	F: CTG AAC TCG CTA AGG CTG CT R: GTT GCG GAC GAT CCA GTA GT	0.1	68
<b>Cathepsin D (TVAG_336300)</b>	F: TAC AAC CCA GAT GCT TTC TC R: GCA TAG ATG TGC CTG TAT CA	0.2	64
<b>Cathepsin B (TVAG_488380)</b>	F: CAA GAG TGC GGT TGT TGC TA R: TAA GCG CAT GCT GTT CAA GA	0.2	60
<b>TvGP63 (GU356538.1)</b>	F: ACG CTG TCC TTG CAA TTC TT R: TTG CGT TTT CTT TTG TGC AT	0.1	60
<b>TvMP50 (TVAG_403460)</b>	F: TCT CGA CTG CGG ATT CTT CT R: TCC GAC GTG ATG AGT CAA AC	0.1	64

### 2.8. Mammalian Cell LDH Release Assay

In order to evaluate the cytolysis capacity of *T. vaginalis* trophozoites pretreated or not with Cu-phendione, an assay was performed to detect lactate dehydrogenase enzyme (LDH) released by cells using Cyto Tox-One homogeneous membrane integrity assay (Promega, USA) reagent. Human vaginal epithelial lineage cells (HMVII) and VERO non-tumoral cell lineage were cultured in RPMI 1640 and DMEM medium, respectively, supplemented with 20% inactive bovine fetal serum and 100 µg/mL penicillin-streptomycin at 37 °C and 5% CO<sub>2</sub>. Prior to the experiment,  $3 \times 10^4$  cells were seeded in 96-well microplates and incubated until monolayer confluence. At this time, ATCC 30236, TV-LACM15, TV-LACM22, and TV-LACH4 were treated with Cu-phendione for 2 h at minimum lethal concentration, as described by Rigo et al. [18]. Afterwards, trophozoites were washed and suspended in RPMI or DMEM medium supplemented with 20% fetal bovine serum and its density adjusted to  $5 \times 10^5$  trophozoites/mL. The control went through the same process; however, only supplemented TYM medium was used during treatment. The

cell medium was removed, then an aliquot of 100  $\mu\text{L}$  of trophozoites was added to the monolayer and incubated for 6 h at 37 °C and 5%  $\text{CO}_2$ . Afterwards, the LDH release was measured according to the manufacturers' instructions. The background value refers to LDH released by cell medium supplemented with 20% inactive bovine fetal serum, while the maximum LDH release is related to cells exposed to 0.2% Triton X-100. The results were calculated using the following formula:

$$\frac{(\text{Experimental Value} - \text{background})}{(\text{Triton X} - 100 - \text{background})} \times 100$$

### 2.9. Statistical Analysis

Experiments were carried out in triplicate and with at least three independent cultures ( $n = 3$ ). The data were expressed by mean  $\pm$  standard deviation. Statistical analysis was performed with GraphPad Prism 8.0.2 using Student's *t*-test, and a significance level of 5% was applied to the data.

## 3. Results and Discussion

### 3.1. Docking Analysis Reveals That Cu-Phendione Interacts with the Active Site of TvMP50, TvGP63, and TvCP2

Considering that phendione has been shown to present activity against *T. vaginalis* cells both when free and when bound to copper or silver metal [18], these three compounds and a prototype MP inhibitor (1,10-phenanthroline) were used for computational analyses. Three-dimensional models of the enzymes were constructed using AlphaFold, as represented in Figures 1–4 (with the aim of evaluating the interaction of the compounds with MPs. The calculated structures have high prediction levels, with pIDDT (Local Distance Difference Test) results greater than 90% (Figure 1A) and 60% (Figure 2A). This test evaluates how well the environment of a reference structure is reproduced in a protein model by calculating the pairs of atoms in the former and the corresponding distance in the latter [32]. The structure of the modeled TvMP50 was submitted to active site identification analysis using Discovery Studio Visualizer v21. Prior to protein characterization analysis, its structure was protonated at pH 6.0 in order to mimic the characteristics of the enzyme in an in vitro environment. As shown in Figures 1B and 2B, it was possible to identify the enzymatic catalytic site (ECS), represented in green. For TvMP50, the ECS was composed of three histidine residues at positions 215, 324, and 335. The amino acids found in the catalytic triad of the model obtained herein were in accordance with the description referring to the family of MP M24 [33]. At the ECS of TvGP63, a glutamic acid residue on position 208 and two histidine residues at positions 207 and 211 can be observed. Furthermore, it was possible to observe a difference in protonation of the enzyme with the increase in pH. As expected, titrable amino acids can change the load according to the alkalization of the medium; however, the coupling capacity of the tested molecules did not change, demonstrating that pH change did not affect the inhibiting action of the test molecules. This result has great relevance, as the dysbiosis caused by the presence of pathogens in the vaginal environment is characterized by pH changes within the range evaluated in this experimental approach.

Subsequently, the interactions between the test compounds and the *T. vaginalis* MPs were investigated by molecular docking analysis. The results revealed that all compounds were able to bind to the active sites of both TvMP50 and TvGP63 MPs (Figure 3, Tables 2 and 3). For TvMP50, Cu-phendione displayed the highest binding affinity ( $-9.7 \text{ kcal}\cdot\text{mol}^{-1}$ ), followed by Ag-phendione ( $-8.8 \text{ kcal}\cdot\text{mol}^{-1}$ ) and phendione ( $-6.1 \text{ kcal}\cdot\text{mol}^{-1}$ ). The same profile was obtained for TvGP63, Cu-phendione having the highest value ( $-10.7 \text{ kcal}\cdot\text{mol}^{-1}$ ) followed by Ag-phendione ( $-8.2 \text{ kcal}\cdot\text{mol}^{-1}$ ) and phendione ( $-6.5 \text{ kcal}\cdot\text{mol}^{-1}$ ). The classical MP inhibitor 1,10-phenanthroline showed a binding affinity of  $-6.0 \text{ kcal}\cdot\text{mol}^{-1}$  against both TvMP50 and TvGP63. It is interesting that the affinity value pattern demonstrated by docking with the MPs was the same as that observed in the anti-*T. vaginalis* action, in which Cu-phendione presented the highest activity against this protozoan [18]. It is relevant that

both 1,10-phenanthroline and Cu-phenadione showed interaction with histidine 335 from the catalytic triad (Figure 3D) of TvMP50; in addition, Cu-phenadione presented interaction of the hydrogen bridge type with the active site (Table 2). All compounds showed interaction with both TvMP50 and TvGP63 active sites; however, Cu-phenadione was chosen for the subsequent assays, as it presented the highest interaction (Figure 3E–H, Tables 2 and 3). In addition, when analyzing the interaction of the Cu-phenadione compound with TvCP2, it has a binding affinity of  $-8.7$  kcal/mol. According to the anchoring position in the TvCP2 structure, the compound interacts with the amino acids TYR210 and VAL174 through hydrophobic interactions, with LYS312 and ASP171 through hydrogen bonds, and with ASP171 through electrostatic interactions (Figure 4, Table 4).

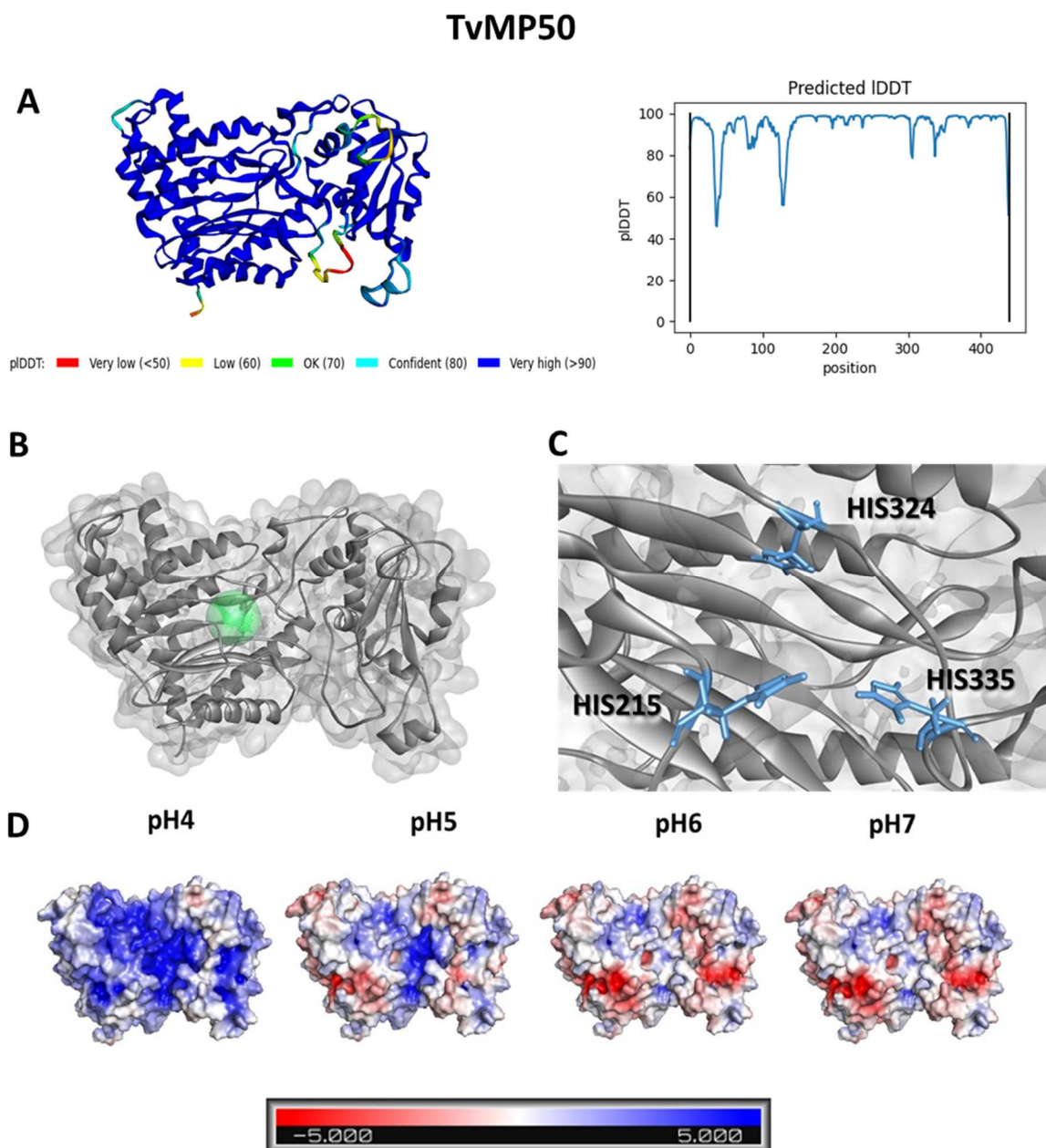


**Figure 1.** Three-dimensional model for TvMP50 of *Trichomonas vaginalis*. (A) PIDD values for the amino acid sequence of the structure modeled using AlphaFold. (B) Active site, represented by the green marking. (C) Identification of amino acids from the enzyme's active site. (D) Electrostatic charge on the surface of the TvMP50 calculated for pH values of 4 to 7. The red-white-blue scale refers to the minimum ( $-5$  kT/e, red) and maximum ( $5$  kT/e, blue) potentials of the surface.

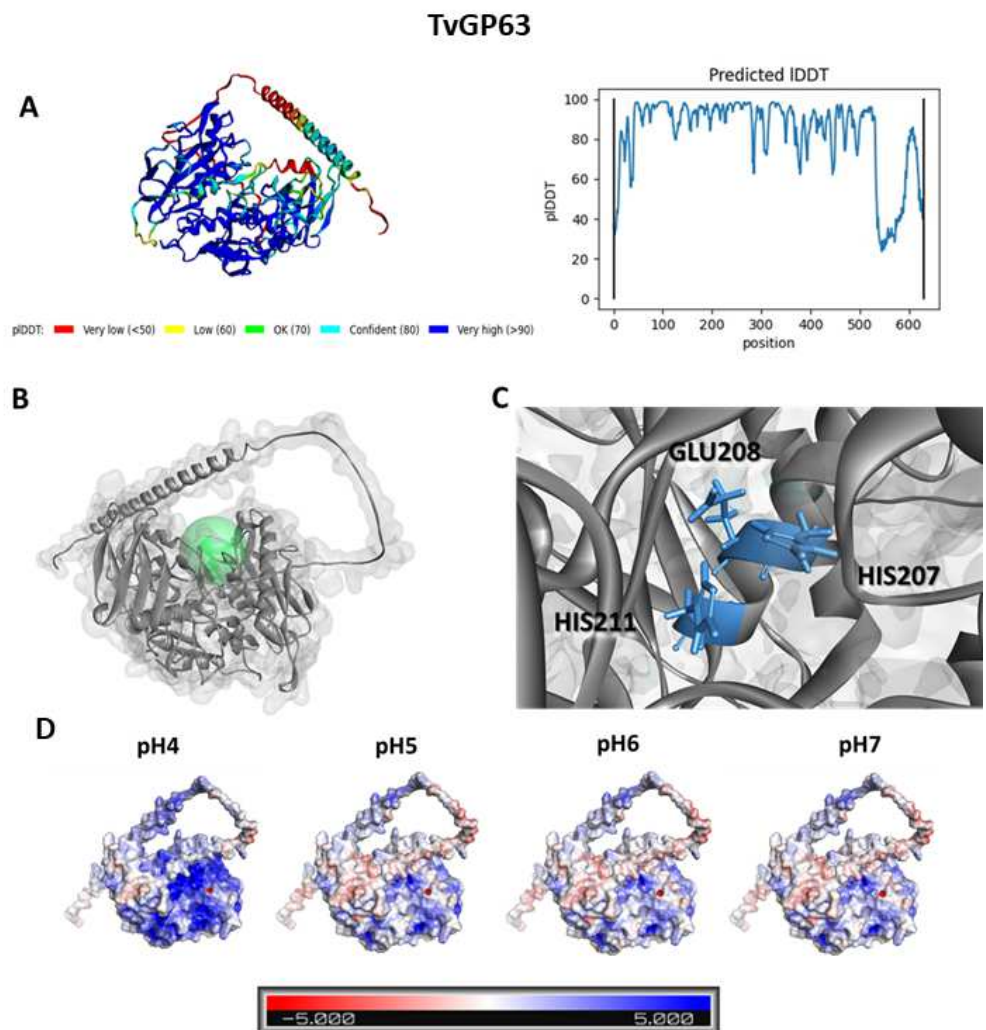


**Figure 2.** Three-dimensional model for TvGP63 of *Trichomonas vaginalis*. (A) PIDDIT values for the amino acid sequence of the structure modeled using AlphaFold. (B) Active site, represented by the green marking. (C) Identification of amino acids from the enzyme's active site (D) Electrostatic charge on the surface of the TvMP50 calculated for pHs 4 to 7. The red-white-blue scale refers to the minimum ( $-5$  kT/e, red) and maximum ( $5$  kT/e, blue) potentials of the surface.

**Table 2.** Docking results predicted by AutoDock Vina: binding affinity, interaction type, amino acid residue, and geometric distance ( $\text{\AA}$ ) for TvMP50 of *Trichomonas vaginalis* with test compounds.

Compounds	Binding Affinity (kcal·mol <sup>-1</sup> )	Interaction Type	Amino Acid	Distance ( $\text{\AA}$ )
1,10-Phenanthroline	-6.0	Hydrogen bonding	ASP232	3.47
			PHE201	4.02
				4.81
		Hydrophobic	HIS335	4.98
			VAL334	5.46
				4.87
Phendione	-6.1	Hydrogen bonding	ASN333	2.02
				2.46
		Hydrophobic	PHE236	4.62
			VAL334	5.18

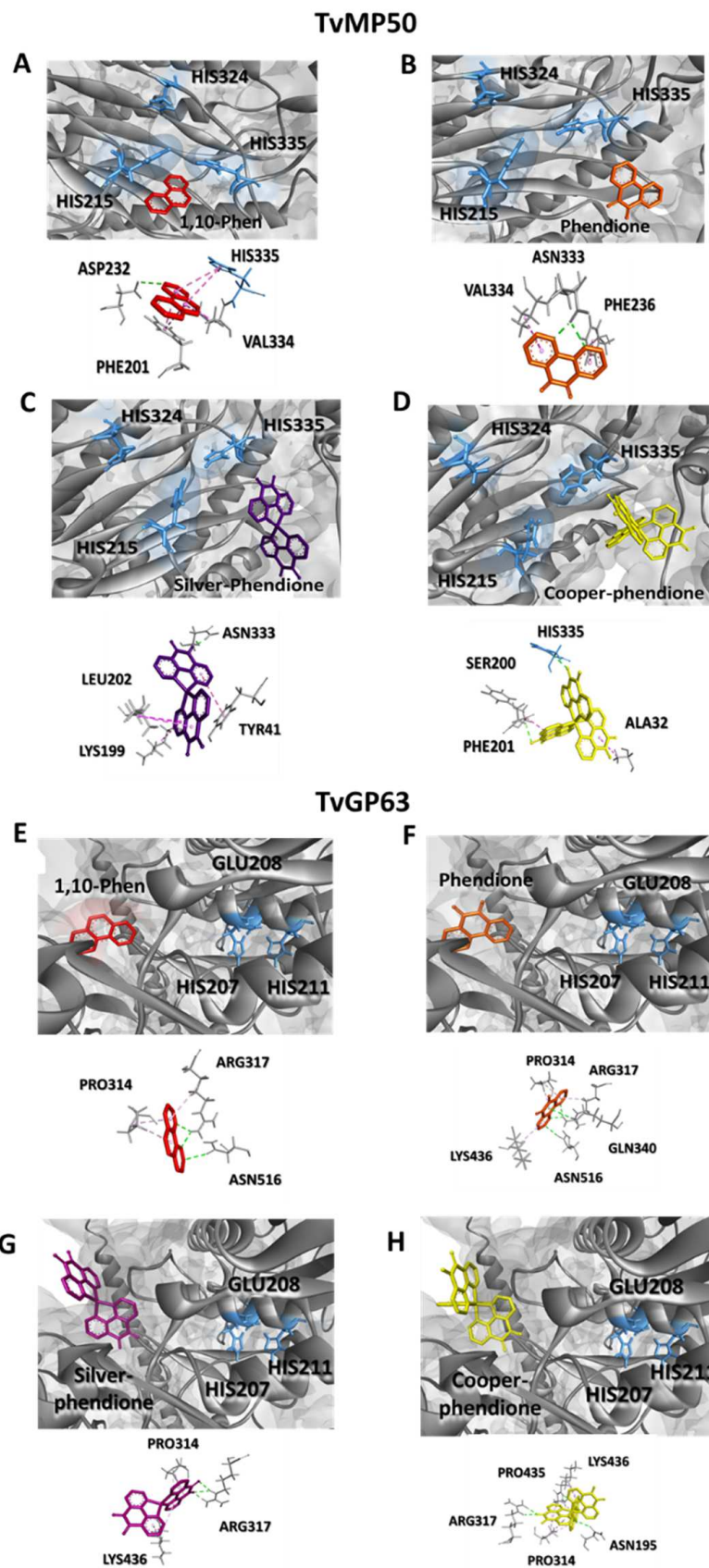


Table 2. Cont.

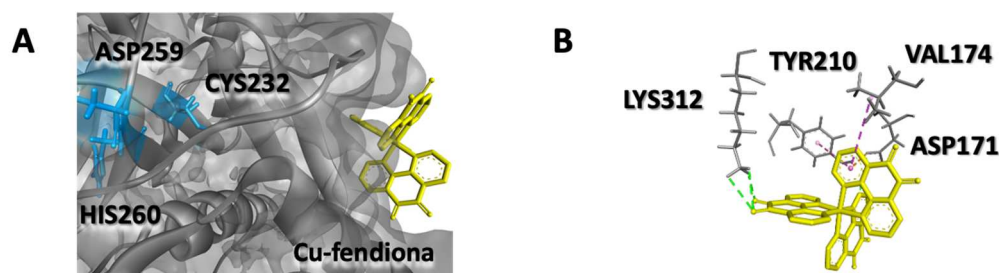
Compounds	Binding Affinity (kcal·mol <sup>-1</sup> )	Interaction Type	Amino Acid	Distance (Å)
Ag-Phendione	−8.8	Hydrogen bonding	ASN333	1.96
				2.99
		Hydrophobic	TYR47	5.22
			LEU202	5.24
			LYS199	5.37
			LEU202	4.68
Cu-phendione	−9.7	Hydrogen bonding	HIS335	2.46
			PHE201	2.49
		Hydrophobic	SER200/ PHE201	4.42
			ALA32	5.29

Table 3. Docking results predicted by AutoDock Vina: binding affinity, interaction type, amino acid residue, and geometric distance (Å) for TvGP63 of *Trichomonas vaginalis* with test compounds.

Compounds	Binding Affinity (kcal·mol <sup>-1</sup> )	Interaction Type	Amino Acid	Distance (Å)
1,10-Phenanthroline	−6.0	Hydrogen bonding	ARG317	2.50
				2.37
			ASN516	3.17
		Hydrophobic	PRO314	4.10
				4.84
			ARG317	4.99
Phendione	−6.5	Hydrogen bonding	ARG317	2.53
				2.43
			ASN516	3.13
		Hydrophobic	GLN340	3.31
			PRO314	5.03
			ARG317	4.15
Ag-Phendione	−8.2	Hydrogen bonding	LYS436	4.98
				5.44
				5.18
		Hydrophobic	ARG317	2.58
				2.62
			LYS436	1.80
Cu-phendione	−10.7	Hydrogen bonding	ARG317	5.00
				5.49
			LYS436	5.18
		Hydrophobic	PRO314	4.25
				5.18
				2.47
Cu-phendione	−10.7	Hydrogen bonding	ARG317	2.13
				3.23
			ASN195	3.04
		Hydrophobic	LYS436	4.40
				4.98
			PRO435	5.41
Cu-phendione	−10.7	Hydrophobic	PRO314	4.81
				4.83
				4.05
		4.89		



**Figure 3.** Docking pose with lower absolute energy ( $\text{kcal}\cdot\text{mol}^{-1}$ ) and 3D interaction diagram of the compounds with the amino acids of TvMP50 and TvGP63 from *Trichomonas vaginalis*. (A,E) 1,10-phenanthroline, (B,F) phendione, (C,G) Ag-phendione, (D,H) Cu-phendione.



**Figure 4.** (A) Docking pose with lower absolute energy ( $\text{kcal}\cdot\text{mol}^{-1}$ ) and (B) 3D interaction diagram of the Cu-phendione with the amino acids of TvCP2 from *Trichomonas vaginalis*.

**Table 4.** Docking results predicted by AutoDock Vina: binding affinity, interaction type, amino acid residue, and geometric distance ( $\text{\AA}$ ) for TvCP2 of *Trichomonas vaginalis* with test compounds.

Compounds	Binding Affinity ( $\text{kcal}\cdot\text{mol}^{-1}$ )	Interaction Type	Amino Acid	Distance ( $\text{\AA}$ )
Cu-phendione	−8.7	Hydrogen bonding	LYS312	2.88
				2.99
				2.34
		Electrostatic	ASP171	3.36
				3.35
				5.41
Hydrophobic	VAL174	5.37		

### 3.2. Cu-Phendione Inhibits the Peptidase Activities of *T. vaginalis*

Considering the interaction of Cu-phendione with the main trichomonad MPs, the effect of this compound in the enzymatic profile was evaluated further. Azocasein is one of the most reliable substrates for measuring proteolytic activity, as it has good color stability and no need for chromogenic reagents [34]. The same methodology used to characterize *T. vaginalis* peptidases has been used to evaluate the trichomonocidal effects of compounds such as 2,4-diamine-quinazoline derivative [27,35]. As shown in Figure 5A, trophozoites treated with Cu-phendione had a significant reduction (77.14%) in their ability to degrade the casein substrate compared to untreated parasite cells, demonstrating an important inhibitory effect on the peptidase pool.

In order to determine the effect of Cu-phendione on different peptidase classes produced by *T. vaginalis*, two fluorogenic peptide substrates were used; Phe-Arg was used to evidence the enzymatic activity of CPs, while MMP was used to measure MPs. As shown in Figure 5B,C, trophozoites treated with Cu-phendione showed a significant reduction in the ability to cleave both peptide substrates, suggesting impairment in the biological functions of these peptidases. An extensive review by Arroyo et al. [9] highlighted the main virulence properties related to CPs, such as cytoskeleton disruption, hemolysis, cytotoxicity, cytoadhesion, immunoglobulin degradation, and induction of host cell apoptosis. MPs are related to pathogenesis of *T. vaginalis* due to the cytotoxic action of these enzymes against host cells, in addition to the immunogenic activity found in the serum of male patients [10,12,36].

The significant reduction of MMP cleavage observed with Cu-phendione was comparable to 1,10-phenanthroline, a well-known MP inhibitor. Studies have already linked the action of Cu-phendione with inhibition of metallo-type enzymes from different clinically relevant microorganisms. Multifunctional elastase B, described as LasB, is an MP from *Pseudomonas aeruginosa* responsible for the degradation of extracellular matrix constituents, potentially leading to tissue injury. Galdino et al. [17] demonstrated that Cu-phendione can interact with the catalytic site of LasB, significantly inhibiting its enzymatic activity. Moreover, MP from *Leishmania* spp. proved to be a target of Cu-phendione, reducing both membrane-associated

and secreted MP activities, with direct impacts on the establishment and maintenance of infection [19]. These results demonstrate an imperative effect of Cu-phendione on cellular homeostasis considering the different functions and MPs enrolled in the protozoal metabolism, leading to in-depth investigation of peptidases targeted by this compound.

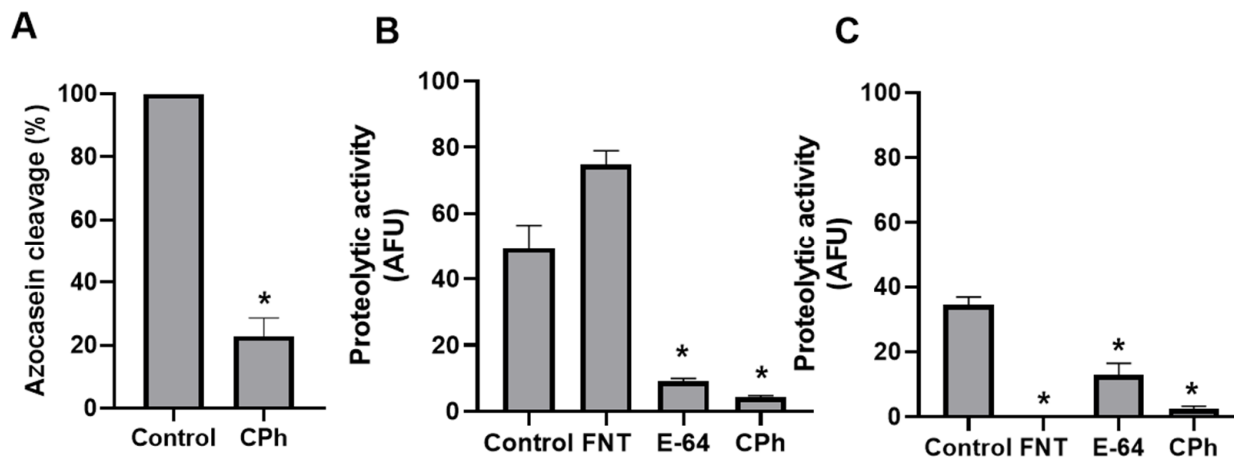


**Figure 5.** Cu-phendione inhibits proteolytic activity in *T. vaginalis*. (A) Azocasein cleavage rate by parasites treated (12.5  $\mu$ M) or not with Cu-phendione (CPh), pH 7.0, 37  $^{\circ}$ C for 90 min. (B) Cleavage of Phe-Arg substrate by parasite lysate at pH 5.0, 37  $^{\circ}$ C for 1 h. Results are expressed as arbitrary fluorescence units (AFU). (C) Cleavage of DNP-Pro-Leu-Gly-Met-Trp-Ser-Arg (MMP) substrate by parasite lysate at pH 9.0, 37  $^{\circ}$ C for 1 h. Results are expressed as arbitrary fluorescence units (AFU). CTL: Untreated control. FNT: 1,10-Phenanthroline. E-64: *L-trans*-epoxysuccinyl-L-leucylamido(4-guanidino) butane. (\*) indicates statistically significant decrease (Student's *t*-test;  $p < 0.05$ ).

### 3.3. Cu-Phendione Negatively Modulates Peptidase Production in *T. vaginalis* Cells

Electrophoresis was performed to identify the nature of enzymes with altered proteolytic activity after treatment. The zymogram in Figure 6 shows regions, with the different shades related to greater or lesser gelatin proteolysis. The dark regions refer to the presence of integral gelatin with greater staining by Coomassie after treatment with Cu-phendione. These regions were excised and analyzed by mass spectrometry and compared to the untreated control, where the enzymes had their proteolytic activity preserved. This methodology is commonly used in the investigation of peptidase activity from *T. vaginalis*. Cathepsin D-like aspartic peptidase, MPs, and several CPs have already had their proteolytic profiles identified by protein gels [13,37–39]. Indeed, this method has been shown to be suitable for comparing the effect of molecules with trichomonocidal action on protozoan peptidases [27].

In order to determine peptidases with reduced activity, the dotted region in the gel was extracted and analyzed by mass spectrometry. Through the UniProt database, 166 protein fragments were identified (Supplementary Material, Table S1); those classified as peptidases according to the UniProt database are grouped in Table 5. TVAG\_387200 was identified as MP-type GP63, while TVAG\_193260 and TVAG\_202060 were identified as CP-type ubiquitin hydrolase, previously identified in the degradome of *T. vaginalis*. Several families can be found in CP, where the CA clan is widely represented by proteins associated with deubiquitinating activity, in addition to the existence of a proteasome pathway linked to ubiquitin in various parasites [4]. Among the main deubiquitinating peptidases in protozoa, the C12 family are represented by ubiquitin terminal hydrolases, which mainly act in ubiquitin recycling when it is erroneously conjugated with intracellular nucleophiles, and the C19 family, which are ubiquitin-specific peptidases that oppose and co-evolve with ubiquitin E3 ligases [40].



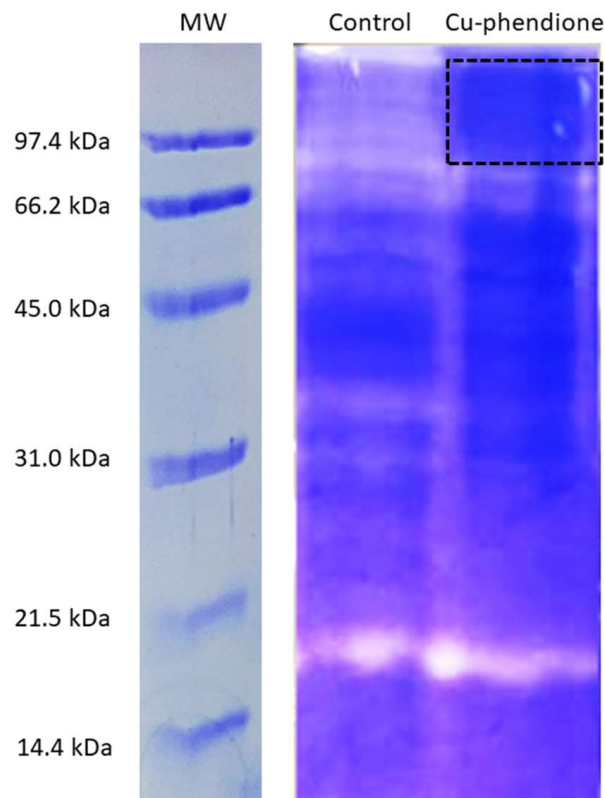


**Figure 6.** Zymogram of the effect of Cu-phendione on *T. vaginalis* peptidases. Peptidase zymograms with gelatin after 24 h of incubation of ATCC 30236 isolate treated or not with Cu-phendione at MIC (12.5  $\mu$ M). The region marked by the square was cut out of the zymogram for gel digestion. MW: Molecular weights in SDS-PAGE without gelatin.

**Table 5.** Peptidases from *Trichomonas vaginalis* found in the band demarcated in the zymogram (Figure S1) and identified by mass spectrometry.

PGLS <sup>a</sup>		UniProt	
Protein Code	Gene	Identification	Molecular Weight
A2G9D4	TVAG_387200	GP63-like	58.572
A2DH40	TVAG_193260	ubiquitin hydrolase-like cysteine peptidase	179.696
A2DWM7	TVAG_202060	Ubiquitin (carboxy-terminal) hydrolase-cysteine peptidase	254.796

<sup>a</sup> Protein Lynx Global Server (PLGS).

### 3.4. Cu-Phendione Modulates the Expression of Peptidase Genes in *T. vaginalis*

Based on the results obtained in the evaluation of peptidase activity, this study investigated the effect of Cu-phendione treatment at the molecular level. To this end, analysis of the mRNA gene expression of the CP, MP, and aspartic peptidase families was performed, starting from the premise that protein synthesis can be activated or repressed under the influence of specific external agents [41]. After treatment with Cu-phendione, the relative expression of mRNA of the *calpain*, *cathepsin L*, *TvMP50*, and *TvGP63* genes showed significant reduction, with particularly emphasis in the MP-related genes. This profile could not be observed for expression of cathepsin types D and B (Figure 7).

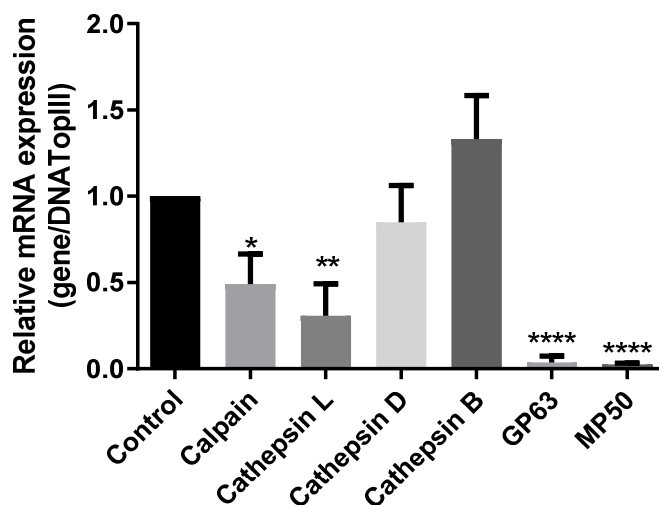


**Figure 7.** Analysis of the mRNA expression of calpain, cathepsin L, cathepsin D, cathepsin B, Gp63, and MP50 relative to the reference gene (*DNATopII*) in *T. vaginalis* treated with Cu-phendione. Statistically significant differences: (\*)  $p < 0.05$ ; (\*\*)  $p < 0.005$ ; (\*\*\*\*)  $p < 0.0001$ .

In fact, Cu-phendione seems to have great importance for the expression of MPs. TvMP50 is part of the M24 family, known as methionyl aminopeptidase. The identification of this enzyme in the protozoan *T. vaginalis* occurred through the gene TVAG\_403460, described as immunogenic only in the serum of male patients [11,36]. Another study confirmed the presence of mRNA of the TVAG\_403460 gene in the isolate T016, referenced in the article by its access number in GenBank, JF263458.1, suggesting that this peptidase is involved in the cleavage of HOST mTOR [13]. The same gene was investigated by Puente-Rivera et al. [10], who demonstrated that the presence of zinc in the microenvironment can promote gene expression and elucidated its location in vesicular structures in the protozoan cytoplasm. In addition, the same study demonstrated that this MP is secreted in its active form and that both forms, secreted and endogenous, exert cytotoxicity against prostate cells, being considered a cytolytic effector involved in the pathogenesis of *T. vaginalis* [10]. In addition, the other MP investigated in this study, TvGP63, is representative of the M8 family. It is described as a zinc-dependent MP, and is not affected by classical inhibitors such as EDTA and phosphoramidon, while 1,10-phenanthroline is active against this MP [3]. Another study described 48 members of TvGP63 family in *T. vaginalis* and separated them into three main groups, -a/-b/-c, with amino acids preserved at position 81 and at positions 515 and 90, and amino acids highly conserved in 75% of TvGP63 sequences. The localization of TVAG\_367130 was described in the plasma membrane, which has great relevance in cytotoxicity processes against cellular hosts [12]. In addition, the occurrence of the *GP63* gene in *T. vaginalis* has been demonstrated and referenced according to GenBank access number GU356538.1, demonstrating that MP acts in the cleavage of the mammalian target of rapamycin (mTOR) of the host cell [13].

### 3.5. Cu-Phendione Reduces the Cytolysis Induced by *T. vaginalis* in Mammalian Cells

Considering the importance of peptidases for *T. vaginalis* cytotoxicity, a cytolysis assay was performed to evaluate whether the pretreatment of trophozoites with Cu-phendione would have any effect in this virulence process. As demonstrated in Table 6, even 2 h of treatment with Cu-phendione was enough to lead to a significant reduction in parasite-mediated cytotoxicity, as observed in both clinical fresh and ATCC reference *T. vaginalis* isolates. In addition, the reduction of cytolysis after Cu-phendione treatment was registered by microscopy of all tested isolates and both mammalian cell lineages (HMVII and VERO) (Supplementary Material, Figures S1 and S2). These results demonstrate that the presence of Cu-phendione can modulate the virulence of *T. vaginalis*.

**Table 6.** LDH release by the HMVII and VERO cell lineages after contact with *Trichomonas vaginalis* <sup>a</sup>.

Treatment Condition	LDH Release (%)	
	HMVII	VERO
Triton X-100	100	100
Tv ATCC 30236	3.8 ± 0.033	7.4 ± 0.217
Tv ATCC 30236 + CPh	0 ± 0.004	0 ± 0.030 *
TvLAC-M22	8.8 ± 0.03	28.6 ± 0.047
TvLAC-M22 + CPh	0 ± 0.01 *	0 ± 0.061 *
TvLAC-M15	9.4 ± 0.010	29.6 ± 0.238
TvLAC-M15 + CPh	0 ± 0.009 *	0 ± 0.113 *
TvLAC-H4	6.7 ± 0.012	29.3 ± 0.010
TvLAC-H4 + CPh	0 ± 0.03 *	0 ± 0.026 *

<sup>a</sup> ATCC 30236, TVLAC-M22, TVLAC-M15 and TV-LAC-H4 isolates treated or not with Cu-phendione (CPh). The data were expressed as a percentage of total lysis, considering Triton X-100 treatment as positive control (100% of LDH release). The data were analyzed by Student's *t*-test, where (\*) *p* < 0.05.

The *T. vaginalis* peptidases participate in several virulence processes against the host, which may vary according to more or less virulent phenotypic isolates. Heterogeneity cytolysis of human vaginal epithelial cells has been determined in different *T. vaginalis* isolates [42]. Arroyo et al. highlighted several virulence properties from CPs, and demonstrated that the cytoadherence and cytotoxicity processes present different levels among *T. vaginalis* isolates, as well as distinct proteolytic activity observed in zymogram profiles [9]. Despite being a complex process that involves the modulation of several pathways of the parasite, the key role of different peptidases in mediating the cytotoxicity process has been increasingly described in the literature. TvCP65 is involved in trichomonad host cellular damage through regulation, probably in the transcriptional and translational levels, with a direct link to the polyamine metabolism [43]. TvCP39 is a glycosylated CP located on the surface the parasite involved in trichomonad cytotoxicity [44]. In addition, MPs have been described as virulence factors. TvMP50 was identified in the cytoplasm and secretion products of trophozoites treated with zinc, and cytotoxicity toward prostatic DU145 cell monolayers was demonstrated [10]. The capacity of lucidin- $\omega$ -isopropyl ether to reduce the cytotoxicity of *T. vaginalis* against HeLa was related to the inhibition of TvMP50 proteolytic activity at the genetic level [45]. In this sense, the inhibition of peptidases by the compound investigated in the present study demonstrates a new option for development of novel anti-*T. vaginalis* agents.

#### 4. Conclusions

Recently, our group demonstrated the effect of Cu-phendione in the oxidative metabolism of *T. vaginalis* due to the decreased function and gene expression of enzymes responsible for detoxification, leading to homeostasis imbalance. Moreover, the Cu-phendione complex led to parasite death by activating an apoptosis-like cell death pathway [20]. Data obtained in the present study suggest that these peptidases are not directly involved in the activation of apoptotic pathways; instead, the multiple targets of Cu-phendione can lead to disturbances in the proteolytic metabolism of the parasite. Moreover, while the compound causes the death of *T. vaginalis* trophozoites by disturbance of the oxidative and proteolytic metabolism, it additionally causes reduced toxic effects against human cells. Indeed, in the scenario where microorganisms are constantly adapting to develop new resistance mechanisms, the presence of a molecule that is able to alter parasite homeostasis by different pathways has a greater ability to circumvent the selective pressure caused by therapy. In this sense, Cu-phendione stands out as a potent antiparasitic molecule able to act in peptidases, with important inhibition capability against *T. vaginalis* MPs.

**Supplementary Materials:** The following supporting information can be downloaded at: <https://www.mdpi.com/article/10.3390/pathogens12050745/s1>, Table S1: Proteins (166) identified by mass spectrometry after zymogram; Figure S1: Light microscopy of cytolysis assay with HMVII lineage after copper-phenidone-treated *Trichomonas vaginalis* isolates ATCC 30236, TV-LACH4, TV-LACM15, TV-LACM22. Cytolysis assay was carried out as described in Material and Methods section. HMVII means cells only; HMVII + Triton X-100: positive control and total disruption of cell monolayer, as expected. In sequence, at the panel left side: each *T. vaginalis* isolate in contact with HMVII cells disrupted the monolayer; at the panel right side: cytolysis was inhibited by Cu-phenidone treatment. Asterisk indicates HMVII cells; arrow indicates *T. vaginalis* trophozoite. Pictures were taken from representative microscopy fields under 400× magnification; Figure S2: Light microscopy of cytolysis assay with VERO lineage after copper-phenidone-treated *Trichomonas vaginalis* isolates ATCC 30236, TV-LACH4, TV-LACM15, TV-LACM22. Cytolysis assay was carried out as described in Material and Methods section. VERO means cells only; VERO + Triton X-100: positive control and total disruption of cell monolayer, as expected. In sequence, at the panel left side: each *T. vaginalis* isolate in contact with VERO cells disrupted the monolayer; at the panel right side: cytolysis was inhibited by Cu-phenidone treatment. Asterisk indicates VERO cells; arrow indicates *T. vaginalis* trophozoite. Pictures were taken from representative microscopy fields under 400× magnification.

**Author Contributions:** Conceptualization, G.V.R., A.L.S.S. and T.T.; Methodology, G.V.R. and F.G.C.; Software, M.M.P.; Validation, G.V.R. and F.G.C.; Formal Analysis, G.V.R.; Investigation, G.V.R., F.G.C. and M.M.P.; Resources, A.L.S.S. and T.T.; Data Curation, T.T.; Writing—Original Draft Preparation, G.V.R.; Writing—Review and Editing, A.L.S.S. and T.T.; Visualization, M.D., M.M., A.L.S.S. and T.T.; Supervision, T.T.; Project Administration, T.T.; Funding Acquisition, M.M.P., A.L.S.S. and T.T. All authors have read and agreed to the published version of the manuscript.

**Funding:** This study was supported by grants from the following Brazilian agencies: Conselho Nacional de Desenvolvimento Científico e Tecnológico (CNPq), Coordenação de Aperfeiçoamento de Pessoal de Nível Superior (CAPES, financial code—001), Fundação de Apoio à Pesquisa do Estado do Rio Grande do Sul (FAPERGS, PPSUS grant 21/2551-0000128-3), and Fundação de Apoio à Pesquisa do Estado do Rio de Janeiro (FAPERJ). G.V.R. thanks CNPq for their fellowship. T.T. thanks CNPq for researcher fellowship grant 309764/2021-1. CIEPQPF is supported by the FCT through the projects UIDB/EQU/00102/2020 and UIDP/EQU/00102/2020.

**Institutional Review Board Statement:** Not applicable.

**Informed Consent Statement:** Not applicable.

**Data Availability Statement:** All of the data generated during the current study are included in the manuscript and/or the Supplementary Data.

**Conflicts of Interest:** The authors declare no conflict of interest.

## References

1. Rowley, J.; Vander Hoorn, S.; Korenromp, E.; Low, N.; Unemo, M.; Abu-Raddad, L.J.; Chico, R.M.; Smolak, A.; Newman, L.; Gottlieb, S.; et al. Chlamydia, gonorrhoea, trichomoniasis and syphilis: Global prevalence and incidence estimates, 2016. *Bull. World Health Organ.* **2019**, *97*, 548–562. [[CrossRef](#)] [[PubMed](#)]
2. Menezes, C.B.; Frasson, A.P.; Tasca, T. Trichomoniasis—Are we giving the deserved attention to the most common non-viral sexually transmitted disease worldwide? *Microb. Cell.* **2016**, *3*, 404–419. [[CrossRef](#)]
3. Rawlings, N.D.; Barrett, A.J.; Thomas, P.D.; Huang, X.; Bateman, A.; Finn, R.D. The MEROPS database of proteolytic enzymes, their substrates and inhibitors in 2017 and a comparison with peptidases in the PANTHER database. *Nucleic Acids Res.* **2018**, *46*, D624–D632. [[CrossRef](#)] [[PubMed](#)]
4. Carlton, J.M.; Hirt, R.P.; Silva, J.C.; Delcher, A.L.; Schatz, M.; Zhao, Q.; Wortman, J.R.; Bidwell, S.L.; Alsmark, U.C.; Besteiro, S.; et al. Draft genome sequence of the sexually transmitted pathogen *Trichomonas vaginalis*. *Science* **2007**, *315*, 207–212. [[CrossRef](#)]
5. Draper, D.; Donohoe, W.; Mortimer, L.; Heine, R.P. Cysteine proteases of *Trichomonas vaginalis* degrade secretory leukocyte protease inhibitor. *J. Infect. Dis.* **1998**, *178*, 815–819. [[CrossRef](#)] [[PubMed](#)]
6. Santos, A.L.S. Protease expression by microorganisms and its relevance to crucial physiological/pathological events. *World J. Biol. Chem.* **2011**, *2*, 48–58. [[CrossRef](#)]
7. Nguyen, T.T.H.; Myrold, D.D.; Mueller, R.S. Distributions of Extracellular Peptidases Across Prokaryotic Genomes Reflect Phylogeny and Habitat. *Front. Microbiol.* **2019**, *10*, 413. [[CrossRef](#)]



8. Štáfková, J.; Rada, P.; Meloni, D.; Žárský, V.; Smutná, T.; Zimmann, N.; Harant, K.; Pompach, P.; Hrdý, I.; Tachezy, J. Dynamic secretome of *Trichomonas vaginalis*: Case study of  $\beta$ -amylases. *Mol. Cell Proteom.* **2018**, *17*, 304–320. [[CrossRef](#)]
9. Arroyo, R.; Cárdenas-Guerra, R.E.; Figueroa-Angulo, E.E.; Puente-Rivera, J.; Zamudio-Prieto, O.; Ortega-López, J. *Trichomonas vaginalis* Cysteine Proteinases: Iron Response in Gene Expression and Proteolytic Activity. *Biomed. Res. Int.* **2015**, *2015*, 946787. [[CrossRef](#)]
10. Puente-Rivera, J.; Villalpando, J.L.; Villalobos-Osnaya, A.; Vázquez-Carrillo, L.I.; León-Ávila, G.; Ponce-Regalado, M.D.; López-Camarillo, C.; Elizalde-Contreras, J.M.; Ruiz-May, E.; Arroyo, R.; et al. The 50kDa metalloproteinase TvMP50 is a zinc-mediated *Trichomonas vaginalis* virulence factor. *Mol. Biochem. Parasitol.* **2017**, *217*, 32–41. [[CrossRef](#)]
11. Arreola, R.; Villalpando, J.L.; Puente-Rivera, J.; Morales-Montor, J.; Rudiño-Piñera, E.; Alvarez-Sánchez, M.E. *Trichomonas vaginalis* metalloproteinase TvMP50 is a monomeric Aminopeptidase P-like enzyme. *Mol. Biotechnol.* **2018**, *60*, 563–575. [[CrossRef](#)] [[PubMed](#)]
12. Ma, L.; Meng, Q.; Cheng, W.; Sung, Y.; Tang, P.; Hu, S.; Yu, J. Involvement of the GP63 protease in infection of *Trichomonas vaginalis*. *Parasitol. Res.* **2011**, *109*, 71–79. [[CrossRef](#)] [[PubMed](#)]
13. Quan, J.H.; Kang, B.H.; Cha, G.H.; Zhou, W.; Koh, Y.B.; Yang, J.B.; Yoo, H.J.; Lee, M.A.; Ryu, J.S.; Noh, H.T.; et al. *Trichomonas vaginalis* metalloproteinase induces apoptosis of SiHa cells through disrupting the Mcl-1/Bim and Bcl-xL/Bim complexes. *PLoS ONE* **2014**, *9*, e110659. [[CrossRef](#)]
14. Viganor, L.; Galdino, A.C.; Nunes, A.P.; Santos, K.R.; Branquinha, M.H.; Devereux, M.; Kellett, A.; McCann, M.; dos Santos, A.L. Anti-*Pseudomonas aeruginosa* activity of 1,10-phenanthroline-based drugs against both planktonic- and biofilm-growing cells. *J. Antimicrob. Chemother.* **2016**, *71*, 128–134. [[CrossRef](#)] [[PubMed](#)]
15. Granato, M.Q.; Gonçalves, D.S.; Seabra, S.H.; McCann, M.; Devereux, M.; dos Santos, A.L.; Kneipp, L.F. 1,10-Phenanthroline-5,6-Dione-Based Compounds Are Effective in Disturbing Crucial Physiological Events of *Phialophora verrucosa*. *Front. Microbiol.* **2017**, *8*, 76. [[CrossRef](#)]
16. Lima, A.K.C.; Elias, C.G.R.; Oliveira, S.S.C.; Santos-Mallet, J.R.; McCann, M.; Devereux, M.; Branquinha, M.H.; Dutra, P.M.L.; dos Santos, A.L.S. Anti-*Leishmania braziliensis* activity of 1,10-phenanthroline-5,6-dione and its Cu(II) and Ag(I) complexes. *Parasitol. Res.* **2021**, *120*, 3273–3285. [[CrossRef](#)]
17. Galdino, A.C.M.; Viganor, L.; Castro, A.A.; Cunha, E.F.F.; Mello, T.P.; Mattos, L.M.; Pereira, M.D.; Hunt, M.C.; O’Shaughnessy, M.; Howe, O.; et al. Disarming *Pseudomonas aeruginosa* Virulence by the Inhibitory Action of 1,10-Phenanthroline-5,6-Dione-Based Compounds: Elastase B (LasB) as a Chemotherapeutic Target. *Front. Microbiol.* **2019**, *10*, 1701. [[CrossRef](#)]
18. Rigo, G.V.; Petro-Silveira, B.; Devereux, M.; McCann, M.; dos Santos, A.L.S.; Tasca, T. Anti-*Trichomonas vaginalis* activity of 1,10-phenanthroline-5,6-dione-based metallo drugs and synergistic effect with metronidazole. *Parasitology* **2018**, *146*, 1179–1183. [[CrossRef](#)]
19. Oliveira, S.S.C.; Santos, V.S.; Devereux, M.; Mccann, M.; Santos, A.L.S.; Branquinha, M.H. The anti-*Leishmania amazonensis* and anti-*Leishmania chagasi* action of copper(II) and silver(I) 1,10-phenanthroline-5,6-dione coordination compounds. *Pathogens* **2023**, *12*, 70. [[CrossRef](#)]
20. Rigo, G.V.; Willig, J.B.; Devereux, M.; McCann, M.; Santos, A.L.S.; Tasca, T. Oxidative damage by 1,10-phenanthroline-5,6-dione and its silver and copper complexes lead to apoptotic-like death in *Trichomonas vaginalis*. *Res. Microbiol.* **2022**, *4*, 104015.
21. Diamond, L.S. The establishment of various trichomonads of animals and man in axenic cultures. *J. Parasitol.* **1957**, *43*, 488–490. [[CrossRef](#)] [[PubMed](#)]
22. McCann, M.; Coyle, B.; McKay, S.; McCormack, P.; Kavanagh, K.; Devereux, M.; McKee, V.; Kinsella, P.; O’Connor, R.; Clynes, M. Synthesis and X-ray crystal structure of [Ag(phendio)<sub>2</sub>ClO<sub>4</sub>] (phendio = 1,10-phenanthroline-5,6-dione) and its effects on fungal and mammalian cells. *Biometals* **2004**, *17*, 635–645. [[CrossRef](#)] [[PubMed](#)]
23. Jumper, J.; Evans, R.; Pritzel, A.; Green, T.; Figurnov, M.; Ronneberger, O.; Tunyasuvunakool, K.; Bates, R.; Žídek, A.; Potapenko, A.; et al. Highly accurate protein structure prediction with AlphaFold. *Nature* **2021**, *596*, 583–589. [[CrossRef](#)] [[PubMed](#)]
24. Martínez-Rosell, G.; Giorgino, T.; de Fabritiis, G. PlayMolecule ProteinPrepare: A Web Application for Protein Preparation for Molecular Dynamics Simulations. *J. Chem. Inf. Model.* **2017**, *57*, 1511–1516. [[CrossRef](#)]
25. Trott, O.; Olson, A.J. AutoDock Vina: Improving the speed and accuracy of docking with a new scoring function, efficient optimization, and multithreading. *J. Comput. Chem.* **2010**, *31*, 455–461. [[CrossRef](#)]
26. Morris, G.M.; Huey, R.; Lindstrom, W.; Sanner, M.F.; Belew, R.K.; Goodsell, D.S.; Olson, A.J. AutoDock4 and AutoDockTools4: Automated docking with selective receptor flexibility. *J. Comput. Chem.* **2009**, *30*, 2785–2791. [[CrossRef](#)]
27. Weber, J.I.; Rigo, G.V.; Rocha, D.A.; Fortes, I.S.; Seixas, A.; de Andrade, S.F.; Tasca, T. Modulation of peptidases by 2,4-diamine-quinazoline derivative induces cell death in the amitochondriate parasite *Trichomonas vaginalis*. *Biomed. Pharmacother.* **2021**, *139*, 111611. [[CrossRef](#)]
28. Bradford, M.M. A rapid and sensitive method for the quantitation of microgram quantities of protein utilizing the principle of protein-dye binding. *Anal. Biochem.* **1976**, *72*, 248–254. [[CrossRef](#)]
29. Martinelli, A.H.; Kappaun, K.; Ligabue-Braun, R.; Defferrari, M.S.; Piovesan, A.R.; Stanisquaski, F.; Demartini, D.R.; Dal Belo, C.A.; Almeida, C.G.; Follmer, C.; et al. Structure-function studies on jaburetox, a recombinant insecticidal peptide derived from jack bean (*Canavalia ensiformis*) urease. *Biochim. Biophys. Acta* **2014**, *1840*, 935–944. [[CrossRef](#)]

30. Rio, D.C.; Ares, M.J.R.; Hannon, G.J.; Nilsen, T.W. Purification of RNA using TRIzol (TRI reagent). *Cold. Spring. Harb. Protoc.* **2010**, *6*, 5439. [[CrossRef](#)]
31. Santos, O.; Rigo, G.V.; Frasson, A.P.; Macedo, A.J.; Tasca, T. Optimal Reference Genes for Gene Expression Normalization in *Trichomonas vaginalis*. *PLoS ONE* **2015**, *10*, e0138331. [[CrossRef](#)]
32. Mariani, V.; Biasini, M.; Barbato, A.; Schwede, T. IDDT: A local superposition-free score for comparing protein structures and models using distance difference tests. *Bioinformatics* **2013**, *29*, 2722–2728. [[CrossRef](#)]
33. Gomis-Rüth, F. Structure and Mechanism of Metalloprotease. *Crit. Rev. Biochem. Mol. Biol.* **2008**, *43*, 319–345. [[CrossRef](#)]
34. Coêlho, D.F.; Saturnino, T.P.; Fernandes, F.F.; Mazzola, P.G.; Silveira, E.; Tambourgi, E.B. Azocasein Substrate for Determination of Proteolytic Activity: Reexamining a Traditional Method Using Bromelain Samples. *Biomed. Res. Int.* **2016**, *2016*, 8409183. [[CrossRef](#)]
35. Hernández, H.; Sariego, I.; Garber, G.; Delgado, R.; López, O.; Sarracent, J. Monoclonal antibodies against a 62 kDa proteinase of *Trichomonas vaginalis* decrease parasite cytoadherence to epithelial cells and confer protection in mice. *Parasite Immunol.* **2004**, *26*, 119–125. [[CrossRef](#)] [[PubMed](#)]
36. Quintas-Granados, L.I.; Villalpando, J.L.; Vázquez-Carrillo, L.I.; Arroyo, R.; Mendoza-Hernández, G.; Alvarez-Sánchez, M.E. TvMP50 is an immunogenic metalloproteinase during male trichomoniasis. *Mol. Cell Proteomics* **2013**, *12*, 1953–1964. [[CrossRef](#)] [[PubMed](#)]
37. Cárdenas-Guerra, R.E.; Arroyo, R.; Rosa de Andrade, I.; Benchimol, M.; Ortega-López, J. The iron-induced cysteine proteinase TvCP4 plays a key role in *Trichomonas vaginalis* haemolysis. *Microbes Infect.* **2013**, *15*, 958–968. [[CrossRef](#)]
38. Carvajal-Gamez, B.I.; Quintas-Granados, L.I.; Arroyo, R.; Vázquez-Carrillo, L.I.; Ramón-Luing, L.L.; Carrillo-Tapia, E.; Alvarez-Sánchez, M.E. Putrescine-dependent re-localization of TvCP39, a cysteine proteinase involved in *Trichomonas vaginalis* cytotoxicity. *PLoS ONE* **2014**, *9*, e107293. [[CrossRef](#)] [[PubMed](#)]
39. Mancilla-Olea, M.I.; Ortega-López, J.; Figueroa-Angulo, E.E.; Avila-González, L.; Cárdenas-Guerra, R.E.; Miranda-Ozuna, J.F.T.; González-Robles, A.; Hernández-García, M.S.; Sánchez-Ayala, L.; Arroyo, R. *Trichomonas vaginalis* cathepsin D-like aspartic proteinase (Tv-CatD) is positively regulated by glucose and degrades human hemoglobin. *Int. J. Biochem. Cell Biol.* **2018**, *97*, 1–15. [[CrossRef](#)] [[PubMed](#)]
40. Atkinson, H.J.; Babbitt, P.C.; Sajid, M. The global cysteine peptidase landscape in parasites. *Trends Parasitol.* **2009**, *25*, 573–581. [[CrossRef](#)] [[PubMed](#)]
41. Jacob, F.; Monod, J. Genetic regulatory mechanisms in the synthesis of proteins. *J. Mol. Biol.* **1961**, *3*, 318–356. [[CrossRef](#)]
42. Bastida-Corcuera, F.D.; Okumura, C.Y.; Colocoussi, A.; Johnson, P.J. *Trichomonas vaginalis* lipophosphoglycan mutants have reduced adherence and cytotoxicity to human ectocervical cells. *Eucaryot. Cell.* **2005**, *4*, 1951–1958. [[CrossRef](#)]
43. Alvarez-Sánchez, M.E.; Carvajal-Gamez, B.I.; Solano-González, E.; Martínez-Benitez, M.; Garcia, A.F.; Alderete, J.F.; Arroyo, R. Polyamine depletion down-regulates expression of the *Trichomonas vaginalis* cytotoxic CP65, a 65-kDa cysteine proteinase involved in cellular damage. *Int. J. Biochem. Cell Biol.* **2008**, *40*, 2442–2451. [[CrossRef](#)] [[PubMed](#)]
44. Ramón-Luing, L.L.; Rendón-Gandarilla, F.J.; Puente-Rivera, J.; Ávila-González, L.; Arroyo, R. Identification and characterization of the immunogenic cytotoxic TvCP39 proteinase gene of *Trichomonas vaginalis*. *Int. J. Biochem. Cell Biol.* **2011**, *43*, 1500–1511. [[CrossRef](#)] [[PubMed](#)]
45. Cáceres-Castillo, D.; Pérez-Navarro, Y.; Torres-Romero, J.C.; Mirón-López, G.; Ceballos-Cruz, J.; Arana-Argáez, V.; Vázquez-Carrillo, L.; Fernández-Sánchez, J.M.; Alvarez-Sánchez, M.E. Trichomonocidal activity of a new anthraquinone isolated from the roots of *Morinda panamensis* Seem. *Drug Dev Res.* **2019**, *80*, 155–161. [[CrossRef](#)] [[PubMed](#)]

**Disclaimer/Publisher’s Note:** The statements, opinions and data contained in all publications are solely those of the individual author(s) and contributor(s) and not of MDPI and/or the editor(s). MDPI and/or the editor(s) disclaim responsibility for any injury to people or property resulting from any ideas, methods, instructions or products referred to in the content.